

## Article

# Mechanical Properties and Thermal Stability of CrZrN/CrZrSiN Multilayer Coatings with Different Bilayer Periods

Hoe-Kun Kim <sup>1</sup>, Sung-Min Kim <sup>2,\*</sup> and Sang-Yul Lee <sup>1,\*</sup>

<sup>1</sup> Center for Surface Technology and Applications, Department of Materials Engineering, Korea Aerospace University, Goyang 10540, Korea; ndkim2@kau.kr

<sup>2</sup> Heat & Surface Technology R&D Department, Korea Institute of Industrial Technology (KITECH), Incheon 21999, Korea

\* Correspondence: sungminkim@kitech.re.kr (S.-M.K.); sylee@kau.ac.kr (S.-Y.L.)

**Abstract:** The CrZrN/CrZrSiN multilayer coatings at a bilayer period range decreasing from 1.35  $\mu\text{m}$  to 0.45  $\mu\text{m}$  were synthesized on a Si (100) wafer and WC-6 wt.% Co substrate using a closed-field unbalanced magnetron sputter, and the thickness effects on the mechanical properties and thermal stability were investigated. The CrZrN/CrZrSiN multilayer coatings showed high hardness and elastic modulus in the ranges of 28 to 33 GPa and 255 to 265 GPa, respectively, and the friction coefficient showed the lowest value of 0.24 on the multilayer coating with a bilayer period of 0.54  $\mu\text{m}$ . The bilayer periods affected the adhesion strength of the multilayer coatings. From the scratch test, the critical load (Lc2) steadily increased with the decreasing of the bilayer period, and the CrZrN/CrZrSiN multilayer coating with a bilayer period of 0.45  $\mu\text{m}$  showed the highest critical load (Lc2) of 79 N. In the case of the annealing test, the bilayer periods affected the thermal stability of the multilayer coatings, and the CrZrN/CrZrSiN multilayer coatings with 0.54  $\mu\text{m}$  showed a maximum hardness value of approximately 30 GPa up to 800 °C.

**Keywords:** CrZrSiN coating; bilayer period; hardness; friction coefficient; adhesion strength



**Citation:** Kim, H.-K.; Kim, S.-M.; Lee, S.-Y. Mechanical Properties and Thermal Stability of CrZrN/CrZrSiN Multilayer Coatings with Different Bilayer Periods. *Coatings* **2022**, *12*, 1025. <https://doi.org/10.3390/coatings12071025>

Academic Editor: Sergey N. Grigoriev

Received: 10 June 2022

Accepted: 17 July 2022

Published: 19 July 2022

**Publisher's Note:** MDPI stays neutral with regard to jurisdictional claims in published maps and institutional affiliations.



**Copyright:** © 2022 by the authors. Licensee MDPI, Basel, Switzerland. This article is an open access article distributed under the terms and conditions of the Creative Commons Attribution (CC BY) license (<https://creativecommons.org/licenses/by/4.0/>).

## 1. Introduction

During the past decade, ternary nitride materials such as TiAlN [1,2], TiZrN [3,4], AlCrN [5,6], and CrZrN [7,8] have been studied to improve tool life due to their excellent mechanical and tribological properties such as high hardness and a low friction coefficient. Recently, transition metal nitride coatings with nanocomposite structure that are defined as a coexistence of the nanocrystalline and amorphous phases with complete immiscibility have emerged [9]. In particular, Si-containing nanocomposite coatings have received much attention due to the incorporation of Si, which led to the grain refinement of the nanocrystalline phase and the formation of amorphous  $\text{Si}_x\text{N}_y$  phase [9–14]. Furthermore, the use of nanocomposites containing Si has been expanded since amorphous  $\text{Si}_x\text{N}_y$  phase suppresses the diffusion of the oxygen ion [15].

Most recently, multilayered hard coatings have gained increasing attention from the industrial and scientific fields because of the enhanced mechanical properties compared to those usually revealed in the corresponding monolithic coatings. As reported in many publications, the multilayer coatings exhibited superior mechanical and tribological properties relative to single-layer hard coatings [16–22]. These improved properties could be attributed to a multilayered structure, consisting of alternating layers with different interface number, composition, and thickness. Generally, multilayer coatings usually show enhanced hardness as the bilayer period decreases. This improved property was attributed to the resistance against dislocation glide across interfaces in multilayer structures [23,24].

From our previous works, the CrZrN coatings showed great mechanical properties such as high hardness (33 GPa), low surface roughness (Rms 0.82 nm), and low friction coefficient (0.25) but relatively poor thermal stability over 500 °C [7,8]. The CrZrSiN

coatings, however, showed moderate hardness (30 GPa) and friction coefficient (0.30), but also excellent thermal stability up to 800 °C [25,26]. Thus, in this work, CrZrN/CrZrSiN multilayer coatings with various bilayer periods were designed and synthesized in order to obtain the coatings with excellent mechanical properties such as hardness, friction coefficient, adhesion properties, and thermal stability. This study provides an insight into the underlying bilayer periods for enhanced mechanical properties and thermal stability of CrZrN/CrZrSiN multilayer coatings.

## 2. Experimental Details

The CrZrN/CrZrSiN multilayer coatings with different bilayer periods were synthesized on two types of substrate, Si (100) wafer and WC-6 wt.% Co substrate, using a closed-field unbalanced magnetron sputtering process. The CrN adhesion interlayer of 300 nm was deposited between the CrZrN/CrZrSiN upper layer and the WC substrate to improve the adhesion, and the bilayer periods were controlled in a range decreasing from 1.35 to 0.45  $\mu\text{m}$ . A pure Cr, Zr, and Si single target (99.99%) was used as target material. Before sputtering, the surface of the Si (100) wafer and WC substrate were cleaned by ultrasonication in acetone for 10 min. After a base pressure was evacuated below  $2.8 \times 10^{-3}$  Pa, the substrates were etched in the presence of Ar plasma for 20 min at a pressure of 0.4 Pa. All the layers were deposited by a pulsed DC power with applied power of 0.5 kW, frequency of 25 kHz, and duty ratio of 70%. The deposition temperature was maintained at 400 °C. The detailed deposition conditions of the CrN interlayer and CrZrN, CrZrSiN upper layers are listed in Table 1.

**Table 1.** Deposition conditions of the CrN interlayer and CrZrN, CrZrSiN upper layers.

Parameters	CrN	CrZrN	CrZrSiN
Base pressure (Pa)	$2.8 \times 10^{-3}$	$2.8 \times 10^{-3}$	$2.8 \times 10^{-3}$
Working pressure (Pa)	$4.2 \times 10^{-1}$	$6.0 \times 10^{-1}$	$6.0 \times 10^{-1}$
Ar gas flow (sccm)	6	15	15
N <sub>2</sub> gas flow (sccm)	10	8	10
Target current (A)	Cr 1.8	Cr 1.2/Zr 1.8	Cr 1.2/Zr 1.6/Si 0.6

The microstructures of the as-deposited coatings were examined by field-emission scanning electron microscopy (FE-SEM, JEOL, JSM-7100F, Tokyo, Japan) operating at an accelerated voltage of 15 kV, and the elemental compositions of individual layers were detected using Oxford Instruments X-Max<sup>N</sup> energy dispersive spectroscopy (EDS). The hardness and elastic modulus of the individual interlayers and coatings were measured using nanoindentation (Helmut Fischer, HM2000, Sindelfingen, Germany) with a load of 25 mN and dwell time of 30 s. Taking into consideration the thickness effect, the indentation depth was maintained at less than approximately 0.16  $\mu\text{m}$ , which was controlled at less than 10% of the total coating thickness [27]. For accurate and reproducible results, both the hardness and elastic modulus tests were carried out 9 times on each sample. The friction coefficient of the coatings was measured using a customized ball-on-disk-type wear tester (Figure 1) with an alumina counter ball (Al<sub>2</sub>O<sub>3</sub>,  $\varnothing = 9.25$  mm). The sliding velocity was 0.25 m/s and the total sliding distance was 1000 m with a normal load of 5 N. The adhesion strength values were evaluated by a scratch tester (CSM, Revetest, Corcelles, Switzerland) with Rockwell C diamond stylus with radius 200  $\mu\text{m}$ , which was drawn across the surface of coatings with a progressively increasing load up to 100 N and a constant sliding speed of 10 mm/min. The critical load (Lc2) and the failure mode of the coatings were determined by observing optical microscopy (Olympus, BX51M, Tokyo, Japan). To evaluate the thermal stability of all the multilayer coatings, annealing was carried out at temperatures ranging from 500 to 800 °C in air for 30 min, and the hardness values of annealed samples were measured using nanoindentation.

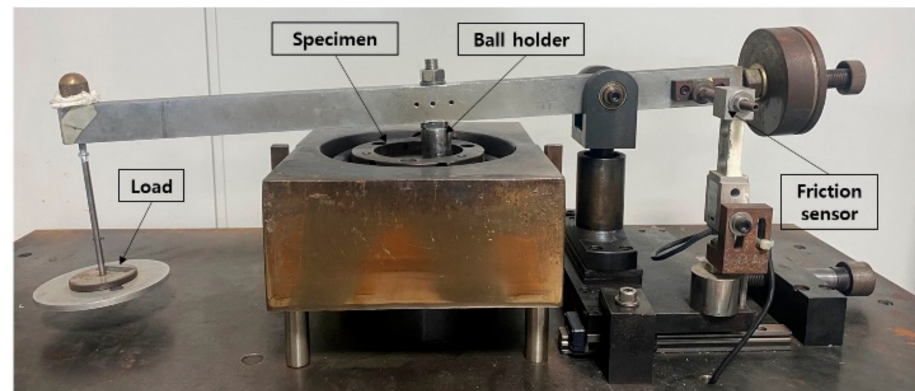


**Figure 1.** Ball-on-disk-type wear tester used for the wear test.

### 3. Results and Discussion

The CrZrN/CrZrSiN multilayer coatings were prepared by varying bilayer periods to enhance their mechanical, tribological, and adhesion properties, and thermal stabilities. As can be seen in the cross-sectional FE-SEM images of the CrZrN/CrZrSiN multilayer coatings (Figure 2), the thickness of all the coatings was adjusted to 3  $\mu\text{m}$  by sputtering duration. In previous work, by means of restructuring the coating with an optimized gradient of the H/E ratio of the WC substrate/CrN interlayer/CrZrN coating, i.e., the minimization of stress gradient between the coating and WC substrate, the adhesion strength was enhanced [28]. Therefore, the CrN interlayer was chosen as the adhesion layer and deposited between the CrZrN/CrZrSiN upper layer and the WC substrate to improve their adhesion strength in this work. Regardless of bilayer periods, the CrZrN in a multilayered structure shows a columnar growth, while the CrZrSiN tends to have a smooth and featureless morphology. However, importantly, with decreasing the bilayer period from 1.35  $\mu\text{m}$  to 0.45  $\mu\text{m}$ , the columnar structure of CrZrN layers transformed from a coarse columnar structure to a dense columnar structure.

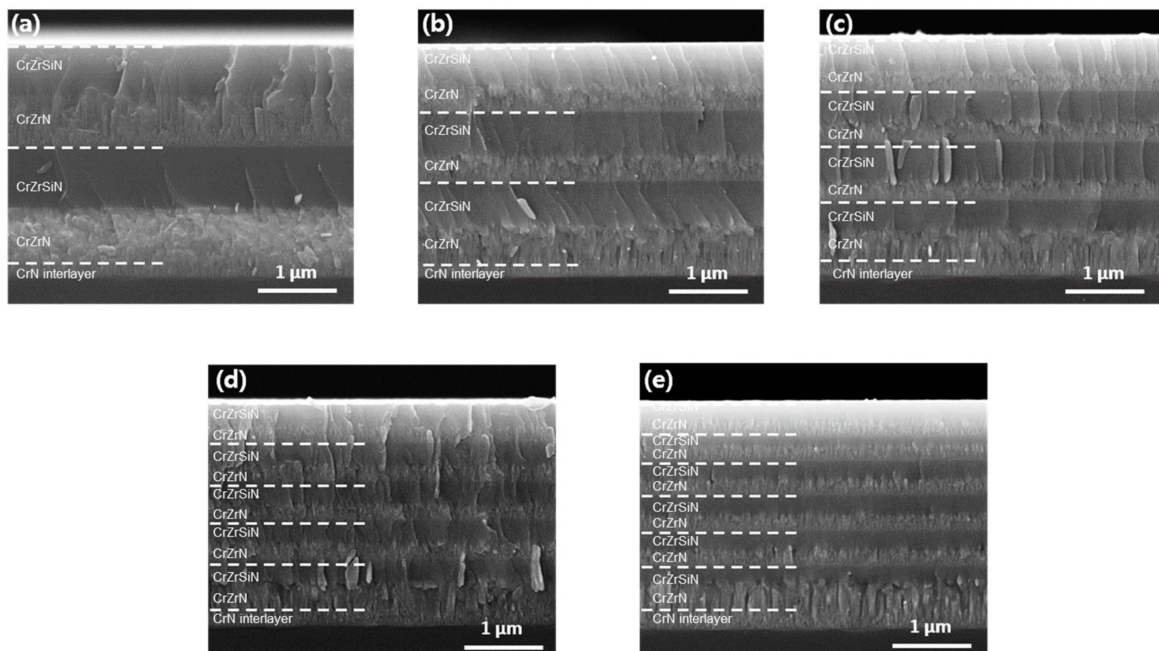


**Figure 2.** Cross-sectional images of the CrZrN/CrZrSiN multilayer coatings with various bilayer periods: (a) 1.35  $\mu\text{m}$ , (b) 0.90  $\mu\text{m}$ , (c) 0.67  $\mu\text{m}$ , (d) 0.54  $\mu\text{m}$ , and (e) 0.45  $\mu\text{m}$ .

The average elemental composition of the WC substrate, CrN interlayer, and CrZrN, CrZrSiN upper layers was measured using SEM-equipped EDS, as summarized in Table 2.

The ratios of non-metallic to metallic elements for all coatings were calculated to be approximately 1.08, which suggests that the ratio of metals to N is almost stoichiometric, 1:1. The hardness (H), elastic modulus (E), and H/E ratio of individual WC substrate, CrN interlayer, and CrZrN, CrZrSiN upper layer are summarized in Table 2, and the hardness and elastic modulus of the CrZrN/CrZrSiN multilayer coatings with various bilayer periods are shown in Figure 3. Both the hardness and elastic modulus increased with the bilayer period decrement. The highest hardness and elastic modulus were approximately 33 and 265 GPa, respectively.

**Table 2.** Elemental compositions, hardness, elastic modulus, and H/E ratio of the WC substrate, CrN interlayer, and CrZrN, CrZrSiN upper layers.

Layer	Composition (at.%)	Hardness (GPa)	Elastic Modulus (GPa)	H/E Ratio
WC substrate	-	19.7 ± 1.6	510.6 ± 8.4	0.045
CrN	48Cr-52N	23.3 ± 1.8	305.6 ± 10.2	0.071
CrZrN	32Cr-16Zr-52N	32.1 ± 1.5	269.3 ± 8.7	0.113
CrZrSiN	21Cr-9Zr-17Si-53N	25.4 ± 1.9	191.5 ± 9.5	0.138

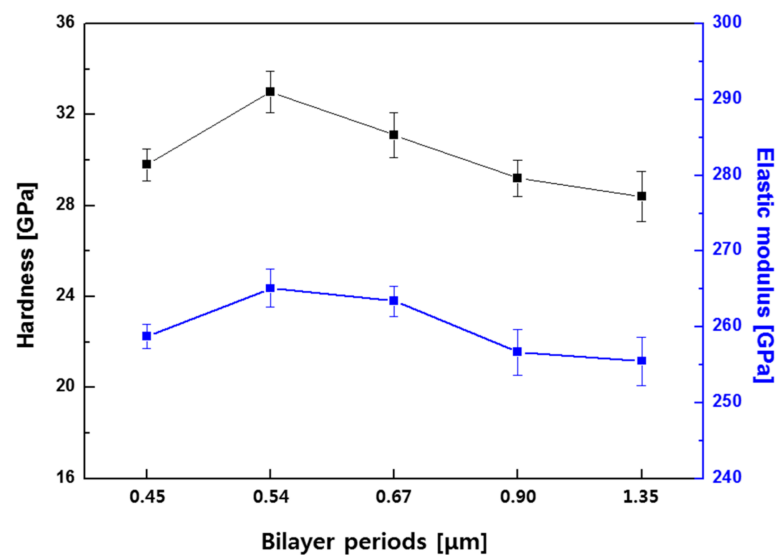


**Figure 3.** The hardness and elastic modulus of the CrZrN/CrZrSiN multilayer coatings with various bilayer periods.

Generally, the multilayered structure of coatings could enhance the hardness on the basis of the dislocation blocking by layer interfaces and lead to the strengthening effect [20,23,24]. The dislocation blocking effect occurred at the interface between layers due to differences in the shear modulus of the individual materials of layers, and the stress required for dislocation glide across interfaces increases. As a result, the high interface density of multilayer structure could contribute to interrupting dislocation glide across the interface between layers. When the bilayer period was decreased to 0.45 μm, however, there was a decrease in the hardness and elastic modulus. These decreased properties could be explained by the loss of the characteristics of a multilayer structure, and the lack of interface effect in the coatings [23,29]. These results show that there is a critical bilayer period of the CrZrN/CrZrSiN multilayer coating required to obtain optimized hardness and elastic modulus.

The friction coefficients of all the CrZrN/CrZrSiN multilayer coatings were evaluated by using the ball-on-disk-type wear tester, and the results are shown in Figure 4. All the friction curves were stable with little variation. It was revealed that the friction coefficient

decreased gradually with the decrease in the bilayer period from 1.35 to 0.54  $\mu\text{m}$ , and the value increased when the bilayer period was 0.45  $\mu\text{m}$ . The coatings with bilayer period of 0.54  $\mu\text{m}$  exhibited the lowest friction coefficient of 0.24, and this follows the same trend as the hardness and elastic modulus of the multilayer coatings.

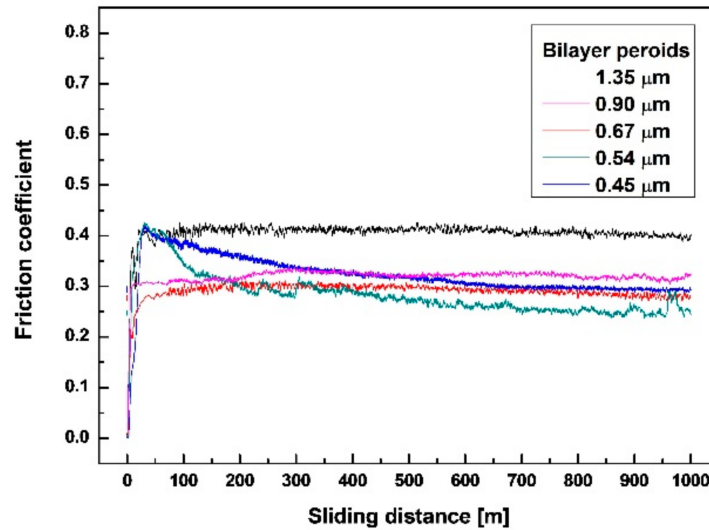


Figure 4. Friction curve of the CrZrN/CrZrSiN multilayer coatings with various bilayer periods.

From the point of view of classical wear theories, the hardness is closely related to the wear resistance of the coating surface. It has been widely accepted that a material with high hardness has high wear resistance. Many reports have also suggested the importance of the elastic modulus correlation with wear behavior [30,31], and wear resistance could be related to the elastic strain to failure of the coating, representing the ability of a material to deform elastically and subsequently recover without plastic deformation. This approach has been applied to the surfaces of coatings, and the elastic strain to failure has been explained by the correlation with the H/E ratio. Therefore, the H/E ratio is a more suitable parameter for predicting the wear resistance of a coating. As can be seen in Figure 5, the highest H/E ratio of the CrZrN/CrZrSiN multilayer coating with a bilayer period of 0.54  $\mu\text{m}$  indicates its best wear resistance, and the friction coefficient of the multilayer coating tends to be proportional to the H/E ratio.

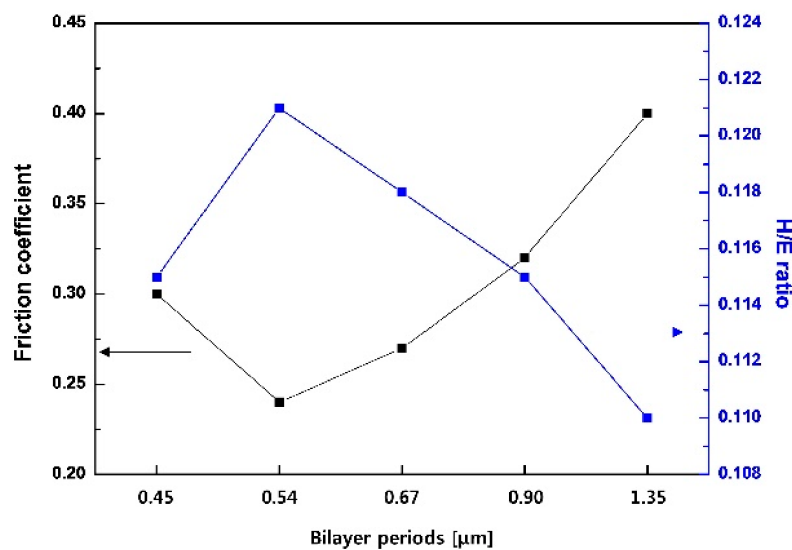
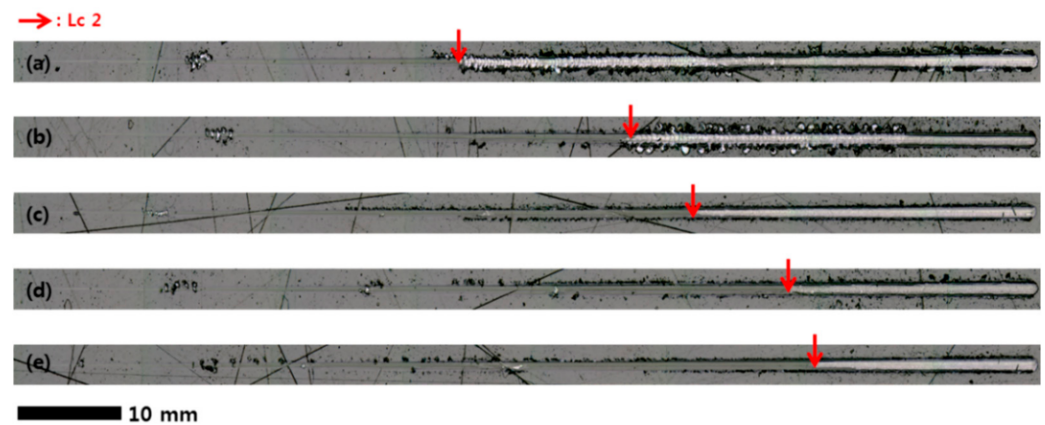


Figure 5. Friction coefficient and H/E ratio as a function of various bilayer periods.

The scratch test provides an informative clue for the adhesion and cohesion properties between a substrate and coating. In the process of a scratch test, three main failures classified as critical load of Lc0, Lc1, and Lc2 are typically derived from a progressive loading on a coating. More specifically, the classification of critical loads is phenomenologically explained as a half-circular crack inside the scratched track induced by plastic deformation (Lc0), an initial fragment or spallation of coating at a track edge (Lc1), and an initial delamination of coating (Lc2) [32,33]. The Lc2 was chosen to comparatively investigate the adhesion strength of the CrZrN/CrZrSiN coating with the different bilayer periods, and the average values calculated from the five measurements made for each coating in this work. The scratch tracks of each coating are shown in Figure 6. It can be observed that the Lc2 increased significantly as the bilayer period decreased from 1.35 to 0.45  $\mu\text{m}$ , and the highest Lc2 was 79 N when the bilayer period was 0.45  $\mu\text{m}$ , as shown in Table 3. In the scratch tracks of the multilayer coating with the bilayer period of 1.35 and 0.90  $\mu\text{m}$ , the chipping cracks were observed and the multilayer coatings were totally delaminated over the Lc2.



**Figure 6.** OM observation from the scratch tracks of the CrZrN/CrZrSiN multilayer coatings with various bilayer periods: (a) 1.35  $\mu\text{m}$ , (b) 0.90  $\mu\text{m}$ , (c) 0.67  $\mu\text{m}$ , (d) 0.54  $\mu\text{m}$ , and (e) 0.45  $\mu\text{m}$ .

**Table 3.** The hardness, elastic modulus, H/E ratio, and critical load (Lc2) of the CrZrN/CrZrSiN multilayer coatings with various bilayer periods.

Bilayer Periods ( $\mu\text{m}$ )	Hardness (GPa)	Elastic Modulus (GPa)	H/E Ratio	Critical Load (Lc2) (N)
1.35	28.4 $\pm$ 2.1	255.5 $\pm$ 7.2	0.110	44
0.90	29.2 $\pm$ 1.7	256.7 $\pm$ 6.7	0.115	60
0.67	31.1 $\pm$ 2.2	263.4 $\pm$ 8.2	0.118	67
0.54	33.0 $\pm$ 2.0	265.1 $\pm$ 7.8	0.121	75
0.45	29.8 $\pm$ 1.9	258.8 $\pm$ 7.3	0.115	79

As reported in the literature [34], the chipping would be often observed in a high hardness coating deposited on the brittle substrate with high hardness. However, there were no obvious chipping cracks or delamination in whole scratch tracks below a bilayer period of 0.67  $\mu\text{m}$ . These improved adhesion properties could be ascribed to the large number of the interfaces in the CrZrN/CrZrSiN multilayer structure [35,36]. During the scratch test, the interfaces in the multilayer coatings played a crucial role as the sites of stress dissipation, and this led to residual stress relaxation and crack propagation prevention in the coating [37]. Therefore, the CrZrN/CrZrSiN multilayer coatings with high density of the interfaces effectively prevented crack propagation during the progressive scratch test, and showed distinctly improved adhesion to the WC substrate with decreasing of the bilayer period.

Figure 7 presents the hardness variation of the CrZrN/CrZrSiN multilayer coatings depending on the bilayer period after annealing at a temperature ranging from 500 to 800 °C in air for 30 min. In all conditions, the hardness values of the multilayer coatings were almost constant above approximately 27 GPa up to 800 °C without drastic change in the hardness, unlike the monolayered CrZrN coating. In addition, the CrZrN/CrZrSiN multilayer coatings exhibited higher hardness compared to the monolithic CrZrSiN coatings even after an annealing process at 800 °C. This means that all the CrZrN/CrZrSiN multilayer coatings showed excellent thermal stability.

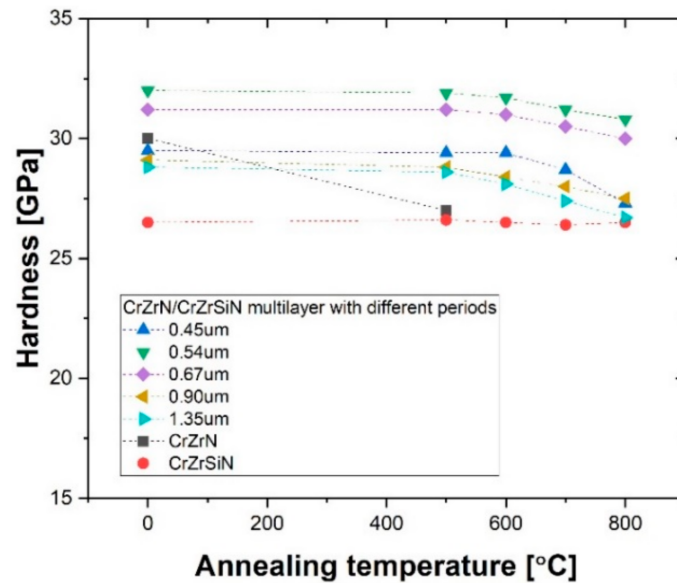


**Figure 7.** Hardness variation of the monolithic CrZrN, CrZrSiN, and multilayered CrZrN/CrZrSiN coatings with various bilayer periods after annealing test in air for 30 min.

Nevertheless, the thermal stability of the multilayer coatings seemed to be influenced by the bilayer periods. It has been well established that the CrZrSiN layer, which consists of  $\text{Si}_x\text{N}_y$  amorphous phase, plays an important role as an oxygen diffusion barrier to inhibit oxidation by residual oxygen during the annealing process, while the CrZrN component is easily oxidized. Interestingly, the hardness change dependent on the bilayer periods was observed after the annealing process, although it was expected that the hardness reduction should be constant due to an almost identical Si content regardless of various bilayer periods. In the case of a bilayer period of 0.45 and 1.35  $\mu\text{m}$ , the hardness decreased approximately 7.4% with increasing annealing temperature from room temperature to 800 °C, relative to the bilayer periods of 0.54, 0.67, and 0.90  $\mu\text{m}$  (3.7–5.5%). This deterioration of thermal stability could be mainly attributed to the structure induced by the bilayer period. Typically, a coarse microstructure of coatings tends to provide the oxygen pathway along the grain boundaries [38]. In addition, the inter-diffusion could occur with the decreased bilayer period, which led to the unexpected monolayered structure [20,21]. Thus, it is believed that the dense microstructure and moderate bilayer period in the range of 0.45–0.90  $\mu\text{m}$  seems to be beneficial to the inhibition of oxygen diffusion and inter-diffusion between layers, leading to improved oxidation resistance.

#### 4. Conclusions

In this work, CrZrN/CrZrSiN multilayer coatings with different bilayer periods were successfully prepared using a closed-field unbalanced magnetron sputtering process on WC-6 wt.% Co substrate to improve their mechanical properties and thermal stability. The hardness and elastic modulus of the CrZrN/CrZrSiN multilayer coatings gradually increased with the decreasing of the bilayer period from 1.35 to 0.54  $\mu\text{m}$ ; however, the values decreased on the multilayer coating with a bilayer period of 0.45  $\mu\text{m}$ . The friction

coefficient followed the same trend as the hardness, and the CrZrN/CrZrSiN multilayer coating with a bilayer period of 0.54  $\mu\text{m}$  showed the lowest friction coefficient of 0.24. The result of the scratch test showed that the adhesion strength increased with the decreasing of the bilayer period, and obvious chipping or delamination were not found when the bilayer period decreased from 0.67 to 0.45  $\mu\text{m}$ . After annealing, the hardness values of all the CrZrN/CrZrSiN multilayer coatings were almost constant above approximately 27 GPa up to 800  $^{\circ}\text{C}$  without drastic change in the hardness, and all the multilayer coatings also showed excellent thermal stability. Therefore, the CrZrN/CrZrSiN multilayer coatings with a moderate bilayer period showed much-improved mechanical properties (hardness, friction coefficient, adhesion) and thermal stability compared to those of each monolithic coating. This work experimentally revealed an optimal period of multilayered coatings for high-performance cutting-tool application.

**Author Contributions:** Conceptualization, H.-K.K.; methodology, H.-K.K.; software, H.-K.K.; validation, H.-K.K. and S.-M.K.; formal analysis, H.-K.K.; investigation, H.-K.K.; resources, H.-K.K.; data curation, H.-K.K.; writing—original draft preparation, H.-K.K.; writing—review and editing, S.-M.K. and S.-Y.L.; visualization, H.-K.K.; supervision, S.-M.K. and S.-Y.L.; project administration, S.-M.K. and S.-Y.L.; funding acquisition, S.-M.K. and S.-Y.L. All authors have read and agreed to the published version of the manuscript.

**Funding:** This study was conducted with the support of the Korea Institute of Industrial Technology as “Development of root technology for multi-product flexible production (KITECH EO-22-0006)”, and this work was supported by a 2022 Korea Aerospace University Faculty Research Grant.

**Institutional Review Board Statement:** Not applicable.

**Informed Consent Statement:** Not applicable.

**Data Availability Statement:** Not applicable.

**Conflicts of Interest:** The authors declare no conflict of interest.

## References

1. Chen, L.; Paulitsch, J.; Du, Y.; Mayrhofer, P.H. Thermal Stability and Oxidation Resistance of Ti-Al-N Coatings. *Surf. Coat. Technol.* **2012**, *206*, 2954–2960. [[CrossRef](#)]
2. Wang, S.; Ji, W.; Wang, Y.; Wei, J.; Qiu, L.; Chen, C.; Jiang, X.; Ran, Q.; Han, R. Comparative Study of Corrosion Behavior of LPCVD-Ti<sub>0.17</sub>Al<sub>0.83</sub>N and PVD-Ti<sub>1-x</sub>Al<sub>x</sub>N Coatings. *Coatings* **2022**, *12*, 835. [[CrossRef](#)]
3. Tung, H.M.; Wu, P.H.; Yu, G.P.; Huang, J.H. Microstructures, Mechanical Properties and Oxidation Behavior of Vacuum Annealed TiZrN Thin Films. *Vacuum* **2015**, *115*, 12–18. [[CrossRef](#)]
4. Volosova, M.; Grigoriev, S.; Metel, A.; Shein, A. The Role of Thin-Film Vacuum-Plasma Coatings and Their Influence on the Efficiency of Ceramic Cutting Inserts. *Coatings* **2018**, *8*, 287. [[CrossRef](#)]
5. Lomello, F.; Sanchette, F.; Schuster, F.; Tabarant, M.; Billard, A. Influence of Bias Voltage on Properties of AlCrN Coatings Prepared by Cathodic Arc Deposition. *Surf. Coat. Technol.* **2013**, *224*, 77–81. [[CrossRef](#)]
6. Warcholinski, B.; Gilewicz, A.; Myslinski, P.; Dobruchowska, E.; Murzynski, D. Structure and Properties of AlCrN Coatings Deposited Using Cathodic Arc Evaporation. *Coatings* **2020**, *10*, 793. [[CrossRef](#)]
7. Kim, S.M.; Kim, B.S.; Kim, G.S.; Lee, S.Y.; Lee, B.Y. Evaluation of the High Temperature Characteristics of the CrZrN Coatings. *Surf. Coat. Technol.* **2008**, *202*, 5521–5525. [[CrossRef](#)]
8. Kim, G.S.; Kim, B.S.; Lee, S.Y.; Hahn, J.H. Structure and Mechanical Properties of Cr-Zr-N Films Synthesized by Closed Field Unbalanced Magnetron Sputtering with Vertical Magnetron Sources. *Surf. Coat. Technol.* **2005**, *200*, 1669–1675. [[CrossRef](#)]
9. Lin, J.; Wang, B.; Ou, Y.; Sproul, W.D.; Dahan, I.; Moore, J.J. Structure and Properties of CrSiN Nanocomposite Coatings Deposited by Hybrid Modulated Pulsed Power and Pulsed Dc Magnetron Sputtering. *Surf. Coat. Technol.* **2013**, *216*, 251–258. [[CrossRef](#)]
10. Diserens, M.; Patscheider, J.; Lévy, F. Mechanical Properties and Oxidation Resistance of Nanocomposite TiN-SiN<sub>x</sub> Physical-Vapor-Deposited Thin Films. *Surf. Coat. Technol.* **1999**, *120–121*, 158–165. [[CrossRef](#)]
11. Mae, T.; Nose, M.; Zhou, M.; Nagae, T.; Shimamura, K. The Effects of Si Addition on the Structure and Mechanical Properties of ZrN Thin Films Deposited by an r.f. Reactive Sputtering Method. *Surf. Coat. Technol.* **2001**, *142–144*, 954–958. [[CrossRef](#)]
12. Xiang, Y.; Zou, C. Effect of Arc Currents on the Mechanical, High Temperature Oxidation and Corrosion Properties of CrSiN Nanocomposite Coatings. *Coatings* **2022**, *12*, 40. [[CrossRef](#)]
13. Liu, Y.; Wang, T.G.; Lin, W.; Zhu, Q.; Yan, B.; Hou, X. Microstructure and Properties of the AlCrSi(O)N Tool Coatings by Arc Ion Plating. *Coatings* **2020**, *10*, 841. [[CrossRef](#)]

14. Chang, L.C.; Zheng, Y.Z.; Chen, Y.I. Mechanical Properties of Zr-Si-N Films Fabricated through HiPIMS/RFMS Co-Sputtering. *Coatings* **2018**, *8*, 263. [[CrossRef](#)]
15. Barshilia, H.C.; Deepthi, B.; Rajam, K.S. Deposition and Characterization of CrN/Si<sub>3</sub>N<sub>4</sub> and CrAlN/Si<sub>3</sub>N<sub>4</sub> Nanocomposite Coatings Prepared Using Reactive DC Unbalanced Magnetron Sputtering. *Surf. Coat. Technol.* **2007**, *201*, 9468–9475. [[CrossRef](#)]
16. Araujo, J.A.; Araujo, G.M.; Souza, R.M.; Tschiptschin, A.P. Effect of Periodicity on Hardness and Scratch Resistance of CrN/NbN Nanoscale Multilayer Coating Deposited by Cathodic Arc Technique. *Wear* **2015**, *330–331*, 469–477. [[CrossRef](#)]
17. Al-Bukhaiti, M.A.; Al-Hatab, K.A.; Tillmann, W.; Hoffmann, F.; Sprute, T. Tribological and Mechanical Properties of Ti/TiAlN/TiAlCN Nanoscale Multilayer PVD Coatings Deposited on AISI H11 Hot Work Tool Steel. *Appl. Surf. Sci.* **2014**, *318*, 180–190. [[CrossRef](#)]
18. Bao, M.; Xu, X.; Zhang, H.; Liu, X.; Tian, L.; Zeng, Z.; Song, Y. Tribological Behavior at Elevated Temperature of Multilayer TiCN/TiC/TiN Hard Coatings Produced by Chemical Vapor Deposition. *Thin Solid Film.* **2011**, *520*, 833–836. [[CrossRef](#)]
19. Ding, X.Z.; Zeng, X.T.; Liu, Y.C. Structure and Properties of CrAlSiN Nanocomposite Coatings Deposited by Lateral Rotating Cathod Arc. *Thin Solid Film.* **2011**, *519*, 1894–1900. [[CrossRef](#)]
20. Kim, S.-M.; Kim, G.-S.; Lee, S.-Y.; Lee, J.-W.; Lee, J.-Y.; Lee, B.-Y. Mechanical Properties and Thermal Stability of CrSiN/AlN Multilayer Coatings Using a Closed-Field Unbalanced Magnetron Sputtering System. *J. Korean Phys. Soc.* **2009**, *54*, 1109–1114. [[CrossRef](#)]
21. Kim, S.; Kim, E.; Kim, D.; La, J.; Lee, S. Effects of Bilayer Period on the Microhardness and Its Strengthening Mechanism of CrN/AlN Superlattice Coatings. *J. Korean Inst. Surf. Eng.* **2012**, *45*, 257–263. [[CrossRef](#)]
22. Bartsch, H.; Grieseler, R.; Mánuel, J.; Pezoldt, J.; Müller, J. Magnetron Sputtered AlN Layers on LTCC Multilayer and Silicon Substrates. *Coatings* **2018**, *8*, 289. [[CrossRef](#)]
23. Zhou, S.Y.; Yan, S.J.; Han, B.; Yang, B.; Lin, B.Z.; Zhang, Z.D.; Ai, Z.W.; Pelenovich, V.O.; Fu, D.J. Influence of Modulation Period and Modulation Ratio on Structure and Mechanical Properties of TiBN/CrN Coatings Deposited by Multi-Arc Ion Plating. *Appl. Surf. Sci.* **2015**, *351*, 1116–1121. [[CrossRef](#)]
24. Chang, Y.Y.; Wu, C.J. Mechanical Properties and Impact Resistance of Multilayered TiAlN/ZrN Coatings. *Surf. Coat. Technol.* **2013**, *231*, 62–66. [[CrossRef](#)]
25. Kim, D.J.; La, J.H.; Kim, K.S.; Kim, S.M.; Lee, S.Y. Tribological Properties of CrZr-Si-N Films Synthesized Using Cr-Zr-Si Segment Targets. *Surf. Coat. Technol.* **2014**, *259*, 71–76. [[CrossRef](#)]
26. Kim, Y.S.; Kim, G.S.; Lee, S.Y. Thermal Stability and Electrochemical Properties of CrZr-Si-N Films Synthesized by Closed Field Unbalanced Magnetron Sputtering. *Surf. Coat. Technol.* **2009**, *204*, 978–982. [[CrossRef](#)]
27. Klemm, S.O.; Schauer, J.C.; Schuhmacher, B.; Hassel, A.W. High Throughput Electrochemical Screening and Dissolution Monitoring of Mg-Zn Material Libraries. *Electrochim. Acta* **2011**, *56*, 9627–9636. [[CrossRef](#)]
28. Kim, H.K.; La, J.H.; Kim, K.S.; Lee, S.Y. The Effects of the H/E Ratio of Various Cr-N Interlayers on the Adhesion Strength of CrZrN Coatings on Tungsten Carbide Substrates. *Surf. Coat. Technol.* **2015**, *284*, 230–234. [[CrossRef](#)]
29. Kot, M.; Rakowski, W.A.; Major, R.; Morgiel, J. Effect of Bilayer Period on Properties of Cr/CrN Multilayer Coatings Produced by Laser Ablation. *Surf. Coat. Technol.* **2008**, *202*, 3501–3506. [[CrossRef](#)]
30. Guo, J.; Wang, H.; Meng, F.; Liu, X.; Huang, F. Tuning the H/E\* Ratio and E\* of AlN Coatings by Copper Addition. *Surf. Coat. Technol.* **2013**, *228*, 68–75. [[CrossRef](#)]
31. Leyland, A.; Matthews, A. On the Significance of the H/E Ratio in Wear Control: A Nanocomposite Coating Approach to Optimised Tribological Behaviour. *Wear* **2000**, *246*, 1–11. [[CrossRef](#)]
32. Bull, S.J.; Rickerby, D.S.; Matthews, A.; Leyland, A.; Pace, A.R.; Valli, J. The Use of Scratch Adhesion Testing for the Determination of Interfacial Adhesion: The Importance of Frictional Drag. *Surf. Coat. Technol.* **1988**, *36*, 503–517. [[CrossRef](#)]
33. Valli, J.; Mäkelä, U.; Matthews, A.; Murawa, V. TiN Coating Adhesion Studies Using the Scratch Test Method. *J. Vac. Sci. Technol. A Vac. Surf. Film.* **1985**, *3*, 2411–2414. [[CrossRef](#)]
34. Bull, S.J. Failure Modes in Scratch Adhesion Testing. *Surf. Coat. Technol.* **1991**, *50*, 25–32. [[CrossRef](#)]
35. Bai, W.Q.; Cai, J.B.; Wang, X.L.; Wang, D.H.; Gu, C.D.; Tu, J.P. Mechanical and Tribological Properties of A-C/a-C:Ti Multilayer Films with Various Bilayer Periods. *Thin Solid Film.* **2014**, *558*, 176–183. [[CrossRef](#)]
36. Voevodin, A.A.; Capano, M.A.; Laube, S.J.P.; Donley, M.S.; Zabinski, J.S. Design of a Ti/TiC/DLC Functionally Gradient Coating Based on Studies of Structural Transitions in Ti-C Thin Films. *Thin Solid Film.* **1997**, *298*, 107–115. [[CrossRef](#)]
37. Holleck, H.; Schier, V. Multilayer PVD Coatings for Wear Protection. *Surf. Coat. Technol.* **1995**, *76–77*, 328–336. [[CrossRef](#)]
38. Kuo, Y.L.; Kencana, S.D. Mechanism of Oxygen Ion Diffusion in Gd-Doped Ceria Electrolyte Films Deposited via Reactive and Direct Sputtering. *Surf. Coat. Technol.* **2017**, *320*, 47–52. [[CrossRef](#)]